Title
Photoemission spectra of CeAl3, CeBe13, CeSi2, and CeCu2Si2: Weights and widths of the 4f emission features

Journal
Physical Review B, 47(23)

ISSN
2469-9950

Authors
Lawrence, JM
Arko, AJ
Joyce, JJ
et al.

Publication Date
1993-06-15

DOI
10.1103/physrevb.47.15460

Photoemission spectra of $CeAl_3$, $CeBe_{13}$, $CeSi_2$, and $CeCu_2Si_2$: Weights and widths of the $4f$ emission features

J. M. Lawrence
Physics Department, University of California, Irvine, California 92717

A. J. Arko, J. J. Joyce, R. I. R. Blyth, R. J. Bartlett, P. C. Canfield, and Z. Fisk
Physics Division, Los Alamos National Laboratory, Los Alamos, New Mexico 87545

P. S. Riseborough
Physics Department, Polytechnic University, Brooklyn, New York 11201
(Received 7 December 1992)

We present valence-band photoemission spectra for $CeAl_3$, $CeBe_{13}$, $CeSi_2$, $CeCu_2Si_2$, and related conventional rare-earth counterpart compounds, taken at photon energies corresponding to the giant $4d$ resonance with resolution ~ 150 meV. We take into account the $5d$ emission, which comprises 30% of the valence-band emission at the $4d$ resonance. We compare the resulting $4f$ emission to the predictions of the Anderson impurity model calculated in a low-order $1/N$ expansion, and including spin-orbit, crystal-field, and finite Coulomb correlation effects. The calculation gives order-of-magnitude fits to the data, but underestimates the spectral weight near the Fermi level by a factor of 2 and overestimates the width of the main f emission at 2 eV by a factor of 4. We argue that Ce photoemission remains an open problem and discuss several experimental and theoretical issues which need to be resolved to make further progress.

I. INTRODUCTION

In this paper we address the question[1-6] of whether the Anderson impurity model adequately describes valence-band $4f$ photoemission in cerium compounds. The comparison is made over the scale of the bandwidth at moderate resolution (150 meV). There are several reasons for undertaking this: our resolution is significantly better than that used in similar earlier studies;[1] in some cases single crystals are now available where older studies were performed on polycrystals; we have made a special effort to subtract the $5d$ emission, which we will argue was done incorrectly in the past; and we have developed a calculation which simultaneously includes spin-orbit and crystal-field splitting, and finite-Coulomb correlation energy.

We present ultraviolet photoemission spectra for four compounds ($CeAl_3$, $CeCu_2Si_2$, $CeSi_2$, and $CeBe_{13}$) chosen so that comparison to theory can be made over two orders of magnitude of Kondo temperature ($T_K = 4$, 8, 40, and 400 K, respectively). The experiments utilized the giant $4d$ resonance at the photon energy $h\nu = 120$ eV to enhance $4f$ emission;[7] the resolution was 150 meV. We estimate the background emission (primarily $5d$) by comparing to spectra of La and Pr compounds taken at their respective $4d$ resonance energies, showing that the $5d$ emission forms an appreciable fraction ($\cong 30\%$) of the $4d$ resonance spectra in these Ce compounds. We then compare the spectra to the predictions of the Anderson impurity model, calculated via the large N expansion method.[1,8] As mentioned, the calculation includes finite Coulomb correlation U, with spin-orbit and crystal-field splittings constrained to their (experimentally) known values. For a fixed background bandwidth W and Coulomb correlation U we then constrain the hybridization $\Delta = V^2\rho$ and the bare f level energy E_f to give the experimentally known Kondo temperature and measured ("renormalized") f level energy $\tilde{E}_f$. The spectra were finally subjected to a degree of broadening equivalent to our experimental instrumental resolution. Our basic findings are that the weight near the Fermi energy (ε_F) observed experimentally is at least two times greater than predicted for the Kondo resonance and its crystal-field and spin-orbit sidebands and that the width of the $f^1 \rightarrow f^0$ emission peak near 2 eV is three to four times smaller in the experimental spectra than predicted.

In the discussion we propose several possibilities to explain these discrepancies between experiment and theory. First, we consider experimental difficulties in determining the bulk $4f$ spectra. These include uncertainties due to our method of subtracting the bulk (mainly $5d$) background; the lack of knowledge of the photon energy dependence of the branching ratio of the $f^1 \rightarrow f^0$ peak to the near-ε_F peak; and the problem of separating out the surface emission. Although the latter is clearly important for 120-eV photoemission spectroscopy (PES), we have not attempted it; but we argue that were we to do so, then in most instances the disagreement between experiment and theory would be worse. We then consider the theoretical difficulties of determining the energy-dependent hybridization $\Delta(\varepsilon) = V^2(\varepsilon)\rho(\varepsilon)$. While use of smaller values of bandwidth W than are expected for these compounds can alleviate the above-mentioned discrepancies somewhat, we argue that the resulting spec-

tra still do not resemble the experimental data in significant respects. The large N approximation scheme may also affect the predictions of the Anderson model. Finally, we discuss the possibility that the discrepancies may arise from a more fundamental source, and that resolution of the difficulties may require (i) inclusion in the model of Coulomb screening of the $4f$ hole, and (ii) recognition that these cerium compounds may be closer to the band limit than implied by the model.[9,10] All of this suggests that photoemission in cerium compounds is an open problem.

II. EXPERIMENTAL TECHNIQUE

The samples consisted of flux-grown single crystals of $CeCu_2Si_2$, $CeBe_{13}$, and $LaBe_{13}$ and arcmelted polycrystals of $PrBe_{13}$, RAl_3 (R=La, Ce, and Pr) and RSi_2 (R=La and Ce). The experiments were performed primarily at the U3C beamline at NSLS; additional experiments were performed at the University of Wisconsin SRC. Both beamlines utilize extended range grasshopper (ERG) monochromators; at lower photon energies at the SRC a Seya monochromator was used. For most of the spectra reported here the photon energy was 116, 120, and 126 eV for the La, Ce, and Pr compounds, respectively, corresponding to the energies of the giant $4d$ resonance for these three elements. An HA-50 hemispherical analyzer coupled to a multichannel detector provided the electron counting. For the $4d$ resonance spectra the total resolution, as determined by numerous measurements of the Fermi edge of Au or Pt, was in the range of 120–180 meV. The samples were cleaved or fractured in an ultrahigh vacuum; the base pressure was in the range $5-10\times10^{-11}$ torr for all experiments. The samples were in direct contact with a Cu cold finger which could be cooled by liquid N_2 ($T\cong80$ K) or liquid He ($T\cong20$ K); a thermocouple attached to the cold finger in close proximity to the sample provided the temperature measurement. Changes in the spectra with temperature were minor. For all the spectra reported here we have subtracted the inelastic background under the conventional assumption that the background at energy E is proportional to the area bounded by the background and the spectrum between E and ε_F.

A problem which plagues the whole area of heavy fermion photoemission is that, with very few exceptions,[11] the samples utilized are polycrystals, and rather poorly characterized by the standards of modern surface science. The spectra can vary somewhat from cleave to cleave and are extremely sensitive to oxidation, which occurs rapidly. Hence, cleanliness and reproducibility are key issues. To study these issues, we cleaved each sample three to six times, under a variety of conditions, and studied the evolution of the spectra with time, as the degree of oxidation increased. As examples of the latter effect we show in Fig. 1 room-temperature spectra of $CeAl_3$ and $CeBe_{13}$, where following the initial spectra the samples were exposed to the base pressure for periods of 6 and 2 h, respectively. It is clear that both the line widths and the fractional weight in the feature near the Fermi level increase markedly with continued exposure. At the same time, a maximum develops near 6-eV binding energy, which is characteristic of O $2p$ emission. For our cleanest spectra, which showed no sign of oxygen emission, we found a smaller degree of cleave dependence, which gives an uncertainty in the linewidths and fractional spectral weights reported below of order 10%. It is worth pointing out that the effects of oxidation and cleave dependence (as well as the uncertainties in determining the background non-$4f$ emission, discussed below) are less of a problem in this study, where our effort is to examine overall features (linewidths and relative spectral weights) at moderate resolution, than for detailed high-resolution studies of the line shape and temperature dependence near ε_F.

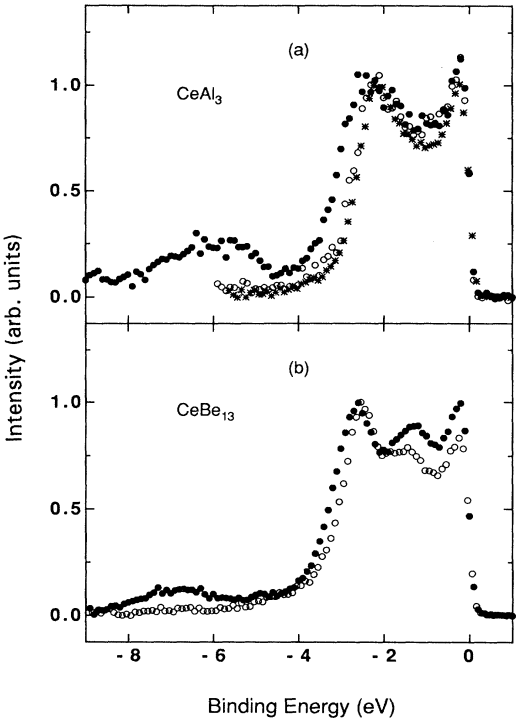

FIG. 1. (a) Valence-band PES of $CeAl_3$ at $h\nu=120$ eV taken with increasing time to show the effect of oxidation on the line shape. Fresh cleave, $T=20$ K, crosses; 4 h after cleave, $T=20$ K, open circles; 6 h after cleave, $T=300$ K, solid circles. (b) Spectra for $CeBe_{13}$ at $h\nu=120$ eV and 300 K. Freshly cleaved sample, open circles; 2 h after cleave, solid circles.

III. EXPERIMENTAL RESULTS AND ANALYSIS

The spectrum of the valence-band region of $CeAl_3$, taken at the giant $4d$ resonance at $h\nu=120$ eV, is shown in Fig. 2(a). Both the $4f$ and $5d$ electrons are known[7] to contribute to this resonance spectrum. To determine the $5d$ contribution, we measured the spectra of the conventional rare-earth counterparts $LaAl_3$ and $PrAl_3$ at their $4d$ resonances at 116 and 126 eV, respectively [Figs. 3(b) and 3(c)]. Simultaneously, we measured the Al $2p$ spectra of all three compounds at the same photon energies [Fig. 3(a)]. All spectra presented are normalized so as to have equal area in the Al $2p$ peak; this assumes that the reso-

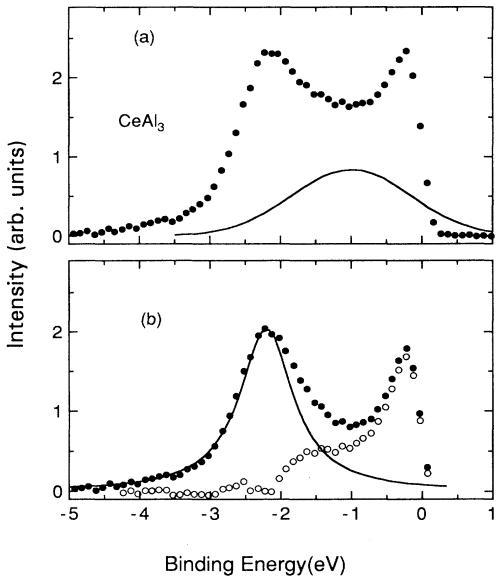

FIG. 2. (a) Valence-band PES of $CeAl_3$ at $h\nu=120$ eV and $T=20$ K. The spectra are normalized to the Al $2p$ emission as described in the text and Fig. 3. The solid line is a Gaussian with the same parameters as for the valence band of $LaAl_3$ [Fig. 3(b)]. (b) The $4f$ emission (solid circles) obtained by subtracting the Gaussian estimate for the $5d$ emission. The solid line, representing the local f^1 peak, is a Lorentzian with binding energy $E_B=2.2$ eV and width (FWHM) 0.92 eV. The open circles are the near-ε_F emission, obtained by subtracting the Lorentzian from the total $4f$ emission.

nance does not affect the emission from the Al core level, and ignores the photon energy dependence of the Al $2p$ emission in the region 116–126 eV. We then fit the valence band of $LaAl_3$ to a Gaussian [Fig. 3(b)]; we assume this represents the $5d$ emission. The spectrum of $PrAl_3$ can be fit to the sum of a Lorentzian representing the Pr $4f$ emission [and whose full width at half maximum (FWHM) is 1.5 eV] and a Gaussian with exactly the same binding energy, width, and height as for $LaAl_3$; this supports the assumption that the $5d$ emission will be essentially identical in all the light rare-earth compounds RAl_3. We thus estimate the $5d$ emission in $CeAl_3$ with precisely the same Gaussian [Fig. 2(a)] noting that the $5d$ emission forms 28% of the total valence-band emission in $CeAl_3$ at 120 eV. After subtracting off the $5d$ emission we obtain our estimate of the $4f$ emission [Fig. 2(b)]. We note that the ratio of the (normalized) $4f$ emission in $PrAl_3$ to that of $CeAl_3$ is 1.8, or approximately 2, as expected since there are twice as many $4f$electrons in Pr as in Ce; this lends added confidence to our procedure. Finally we fit the $4f$ emission in $CeAl_3$ to the sum of a Lorentzian, representing emission from a local $4f$ state, which we call the "$4f^1\rightarrow 4f^0$" emission, and a remainder, which we label as the "near-ε_F" emission. The $4f^1\rightarrow 4f^0$ peak has a width (FWHM) of 0.9 eV; the fractional weight in the near-ε_F emission is 37%.

The $4d$ resonance spectra of $LaSi_2$ and $CeSi_2$, normalized to equal area in the Si $2p$ peaks [Fig. 4(a)] are shown in Fig. 4(b). The $LaSi_2$ spectrum has an area equal to 30% of the total $CeSi_2$ spectrum; this is very close to the value 28% for the $5d$–valence-band fraction given above for $CeAl_3$ and increases our confidence that the $LaSi_2$ spectrum can be taken as the $5d$ emission in $CeSi_2$, and is appropriately normalized. After subtracting the $5d$ emission we obtain the $4f$ emission in $CeSi_2$ [Fig. 4(c)]; this is again fit to the sum of a Lorentzian, representing the $4f^1\rightarrow 4f^0$ peak, and a remainder. This latter near-ε_F peak has a fractional area of 33%; the $4f^1\rightarrow 4f^0$ peak has a width (FWHM) of 1.5 eV.

Additional information concerning the background emission can be obtained by studies at photon energies below the threshold for the onset of f emission; such spectra are often taken as representing the background emission from $5d$ and other (e.g., Si $3p$) states. In Fig. 5 we compare such spectra for $LaSi_2$ and $CeSi_2$, taken at 26 eV, to the spectra of $LaSi_2$ taken at the $4d$ resonance (116 eV) and of $CeSi_2$ taken at the Fano minimum of the $4d$ resonance (112 eV). Both pairs of spectra have three peaks (at −4, −2, and 0 eV) but the branching ratios of

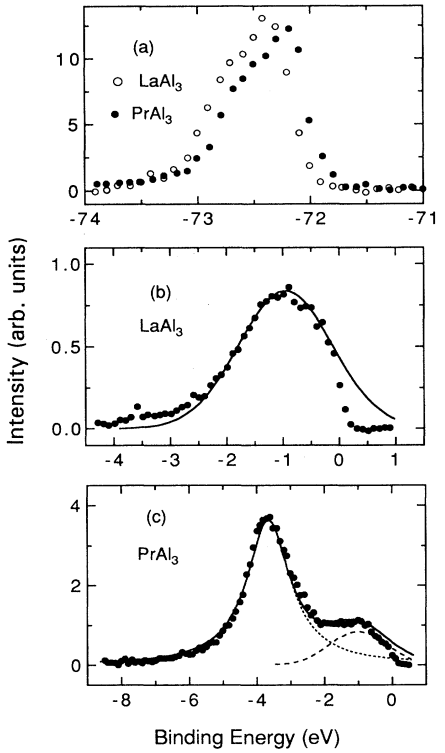

FIG. 3. (a) The Al $2p$ core levels of $LaAl_3$ and $PrAl_3$ at $h\nu=116$ and 126 eV, respectively, and $T=300$ K. The spectra are normalized to have the same area. (b) The valence band of $LaAl_3$ at $h\nu=116$ eV, normalized to the Al $2p$ core level. The solid curve is a Gaussian approximation to the emission; with binding energy $E_B=1.0$ eV, standard deviation $\sigma=0.83$ eV and height 0.84. (c) The valence band of $PrAl_3$, normalized to the Al $2p$ core level, at $h\nu=126$ eV and $T=300$ K. The long-dashed line, representing the $5d$ emission, is a Gaussian with the same parameters as for $LaAl_3$; the short-dashed line, representing the $4f$ emission, is a Lorentzian with $E_B=3.65$ eV and width (FWHM) 1.52 eV.

the three peaks are clearly different at the two photon energies; in particular the peak near the Fermi edge is enhanced and the peak at 4 eV is suppressed in the 26-eV spectra. These differences arise from relative changes in the optical-absorption matrix elements for the three peaks as the photon energy varies. Since our $CeSi_2$ valence-band spectrum was obtained at $h\nu=120$ eV, it is clearly more appropriate to determine the strength of the $5d$ emission at an approximately equal photon energy (as we have done by use of the $LaSi_2$ $4d$ resonance spectrum) than at the lower energies ($h\nu=20-30$ eV).

We did not measure a core level for normalization in the RBe_{13} series. Instead, we proceeded as follows: We measured the $LaBe_{13}$ spectrum at the $4d$ resonance, and the spectra of $CeBe_{13}$ and $PrBe_{13}$ at a low photon energy (27 eV) chosen to lie below the threshold for the onset of f emission [Fig. 6(a)]. All three spectra have the same three-peaked structure and furthermore the branching ratios are the same at both photon energies; hence, we take the $5d$ emission as proportional to the $LaBe_{13}$ spectrum, but with as yet undetermined overall scale factor. Two ways to choose the scale factor are shown in Fig. 7 for $CeBe_{13}$. In the top panel we have chosen the scale factor to be sufficiently large that when $5d$ is subtracted there is no trace of the middle peak near 1.5-eV binding energy, which is the peak that corresponds to the largest peak in the $5d$ emission. In doing this, however, we find that the resulting $5d$ emission is nearly 50% of the total valence-band emission in $CeBe_{13}$ and the resulting fractional weight in the near-ε_F emission is only 11% of the $4f$ emission, as opposed to the values of 30% and 35% observed in $CeAl_3$ and $CeSi_2$. In the lower panel we have chosen the scale factor so that the $5d$ emission is 30% of the valence band. For this choice, after subtraction of the $4f^1\rightarrow 4f^0$ Lorentzian (FWHM=1.2 eV), the remaining near-ε_F emission has a fractional weight of 28%, now comparable to that for $CeAl_3$ and $CeSi_2$. We take the latter choice of the $5d$ emission as the more probable. We have also attempted to determine the correct choice of scale factor for $PrBe_{13}$. However, for this compound the valence-band spectra cannot be neatly decomposed into the sum of a Lorentzian plus the $5d$ emission, as for $PrAl_3$. The choice of $5d$ emission shown in Fig. 6(b) has the virtue that it fits the Fermi edge very well; a greater choice of scale factor would overestimate the emission at ε_F. It leads to the result, however, that there is a large remaining peak [the long-dashed line in Fig. 6(b)] in the valence band of $PrBe_{13}$.

The spectra of $CeCu_2Si_2$ at the $4d$ resonance ($h\nu=120$ eV) as well as off-resonance ($h\nu=112$ eV) are shown in

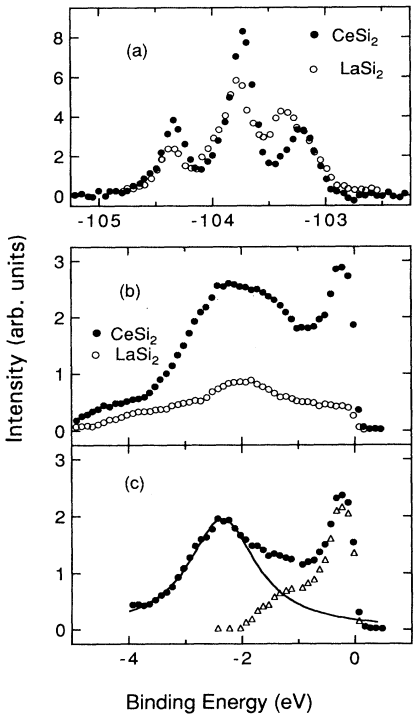

FIG. 4. (a) Si sp core levels, normalized to equal area, for $LaSi_2$ ($h\nu=116$ eV, $T=80$ K) and $CeSi_2$ ($h\nu=120$ eV, $T=20$ K). (b) Valence-band spectra, normalized to the Si $2p$ core levels, for $CeSi_2$ ($h\nu=120$ eV, $T=20$ K) and $LaSi_2$ ($h\nu=116$ eV, $T=80$ K). (c) $4f$ emission for $CeSi_2$ (solid circles), obtained by subtraction of the $LaSi_2$ emission. The local f^1 peak is represented as a Lorentzian with binding energy $E_B=2.35$ eV and FWHM 1.46 eV. The open triangles are the near-ε_F emission, obtained by subtracting the Lorentzian.

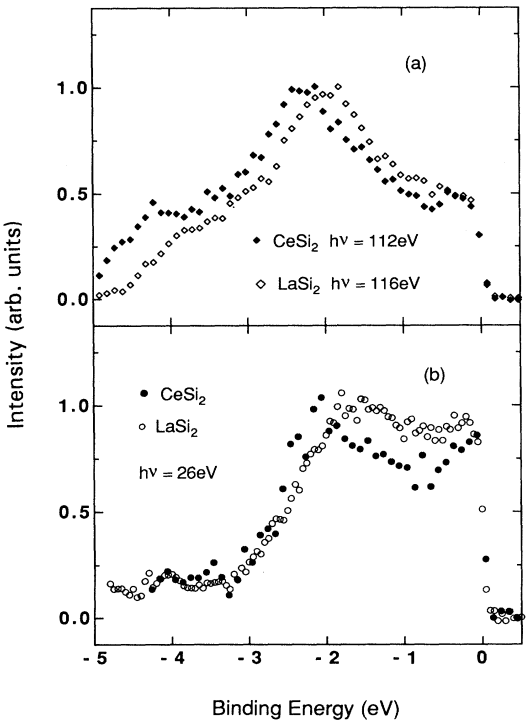

FIG. 5. (a) Off-resonance spectrum for $CeSi_2$ ($T=20$ K) and on-resonance spectrum for $LaSi_2$ ($T=80$ K). (b) Spectra for $CeSi_2$ (20 K) and $LaSi_2$ (80 K) taken below the threshold ($h\nu=30$ eV) for the onset of f emission. This figure shows two methods of estimating the $5d$ emission, but demonstrates that the branching ratios between the three peaks in the $5d$ spectra vary with photon energy. (All spectra are normalized to unit height near 2 eV.)

Fig. 8(a); the spectra are normalized to unity at the copper $3d$ peak at 4 eV. For this case we do not at present have data for the La counterpart, so we proceed as follows. An examination of Fig. 8 shows a clear peak near 1.67 eV in both the on- and off-resonance spectra. In Fig. 8(b) we fit the off-resonance data in the interval 3.5 eV below the Fermi level to the sum of a Lorentzian representing the tail of the Cu peak at 4 eV, a second Lorentzian for the peak at 1.67 eV, and a reversed arctangent for the Fermi step. We then assume that the emission in the Fermi step and the peak at 1.67 eV represent the $5d$ emission, and hence at resonance will be enhanced to a magnitude equal to 30% of the total emission in the valence band, as for the other compounds. To determine the $4f$ emission, we first subtract the peak representing the copper emission from the on-resonance data, assuming that it should not resonate. We then scale the sum of the peak at 1.67 eV and the Fermi step so that its weight is 30% of the resulting valence-band emission. The $4f$ emission obtained after subtraction [Fig. 9(a)] shows no hint of the peak at 1.67 eV. The resulting $4f^1 \rightarrow 4f^0$ peak has a width 1.12 eV (FWHM) and the near-ε_F peak comprises 49% of the total $4f$ emission.

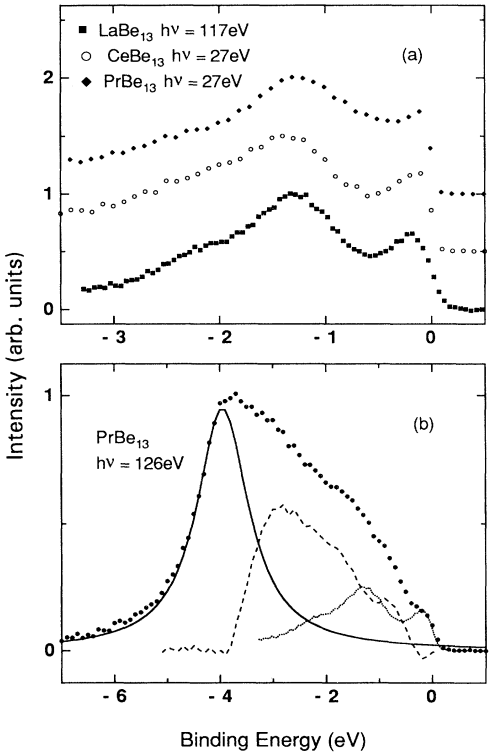

FIG. 6. (a) Un-normalized spectra for $LaBe_{13}$ taken on resonance (300 K) and for $CeBe_{13}$ (20 K) and $PrBe_{13}$ (80 K) taken below the threshold for $4f$ emission. For this material the branching ratio for the non-$4f$ emission appears to be constant with photon energy. (b) Spectrum for $PrBe_{13}$ taken on resonance. The dotted curve, proportional to the curves in (a), and normalized as discussed in the text, represents the non-$4f$ emission. The Lorentzian ($E_B = 3.9$ eV, FWHM = 1.20 eV) represents the local $f^2 \rightarrow f^1$ peak. The long-dashed curve is the extra $4f$ emission.

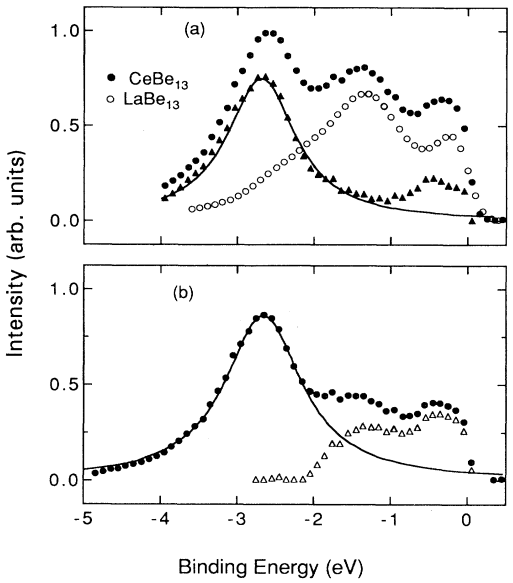

FIG. 7. (a) The on-resonance spectrum of $CeBe_{13}$ ($h\nu = 120$ eV, $T = 20$ K) and $LaBe_{13}$ ($h\nu = 117$ eV, $T = 300$ K). The latter is normalized so that when subtracted, no vestige of the peak near 1 eV remains in the $4f$ spectra (solid triangles). (b) $4f$ emission for $CeBe_{13}$ (solid circles) obtained by subtracting the $LaBe_{13}$ spectrum, normalized so as to give the same fraction of $5d$ emission on resonance as in $CeAl_3$ and $CeSi_2$. For reasons stated in the text, we believe this is a better method of normalizing than in (a). The parameters of the Lorentzian (solid line) are $E_B = 2.6$ eV, FWHM = 1.2 eV. The remainder after subtracting the Lorentzian is the near-ε_F emission (open triangles).

(Variants on our procedure, i.e., other choices of the ratio of the weight in the peak at 1.67 eV to the weight in the Fermi step, give similar final results for the near-ε_F weight and $f^1 \rightarrow f^0$ width.)

IV. THEORETICAL METHODS

The photoemission spectrum was fit using the results of a variational $1/N$ expansion for the single-impurity Anderson model. The calculational method used was that of Refs. 12 and 13. We will give full details in a future review; here we focus on similarities and differences between our calculation and those of Refs. 12 and 13. The calculation included the effects of splitting the full fourteenfold degeneracy of the $4f^1$ configuration by spin-orbit and crystal-field interactions. That is, we consider f^1 multiplets $\{\alpha\}$ with energies $E_{f\{\alpha\}}$ and degeneracies $N_{\{\alpha\}}$. The restriction to the $U \rightarrow \infty$ limit of the Anderson model was partially lifted by including states incorporating the f^2 configuration into the set of variational basis states. (To the best of our knowledge, this is the first calculation of photoemission spectra using a $1/N$ treatment of the Anderson model to simultaneously include crystal-field, spin-orbit, and finite-U effects.) The f^2 configuration was assumed *not* to be split by spin-orbit and crystal-field interactions. The hybridization matrix elements were assumed to be independent of the particular f^1 multiplet $\{\alpha\}$ involved, and also independent of energy. The variational basis states used for the ground-

state wave function consisted of those specified in Eqs. (3.1), (3.2), and (3.4) of Ref. 12, which incorporate terms of leading order in $1/N$.

A set of coupled equations for the variational coefficients for the ground-state wave function and the ground-state energy were found. These were reduced to an integral equation for an amplitude $a_{\mathbf{k},\{\alpha\}}$ which, when solved, yields a transcendental equation for the ground-state energy. This procedure is analogous to that used in Refs. 12 and 13. The integral equation [see Eq. (4.3)] is not separable, except in the $U \rightarrow \infty$ limit. Following the procedure outlined in Ref. 13 [see Eq. (4.6)], the integral equation can be decoupled by neglecting the kinetic-energy dependence of the denominator. This approximation is expected to be reasonable in the large U limit, i.e., $U \gg W$. (For the purposes of fitting spectra in real materials, other authors[1,8] have solved the integral equation numerically, without resort to this approximation. We argue, however, that use of this decoupling procedure should lead to no greater inaccuracy than the neglect of configurations f^n with $n > 2$.) Unlike the $N = 14$ case, the resulting transcendental equation for the bound-state energy [a generalization of Eq. (4.7) of Ref. 13] may possess more than one solution. The lowest energy solution corresponds to the ground-state energy.

In the variational ground state, the Kondo singlet is formed by binding a conduction electron to an electron predominantly in the lowest f^1 multiplet. The resulting complex, consisting of a local f moment and the screening electron, produces a nonmagnetic singlet. The higher energy solutions of the integral equation, when they exist, also correspond to a Kondo singlet in which the f^1 configuration is a superposition consisting mostly of the higher multiplets. These excited spin-orbit and crystal-field-split Kondo states have characteristic binding energies or Kondo temperatures T_K^* which are different[2] from the ground-state Kondo temperature T_K. These higher energy Kondo singlets and the resulting features in the photoemission spectra are well separated when the splittings between f^1 multiplets are greater than the relevant Kondo temperatures.

In the sudden approximation, the zero-temperature limit of the photoemission spectrum is approximated by the density of states for removal of one f electron. The matrix element of the resolvent, taken between states where one f electron has been removed, is calculated by a method analogous to that of Ref. 13. The appropriate

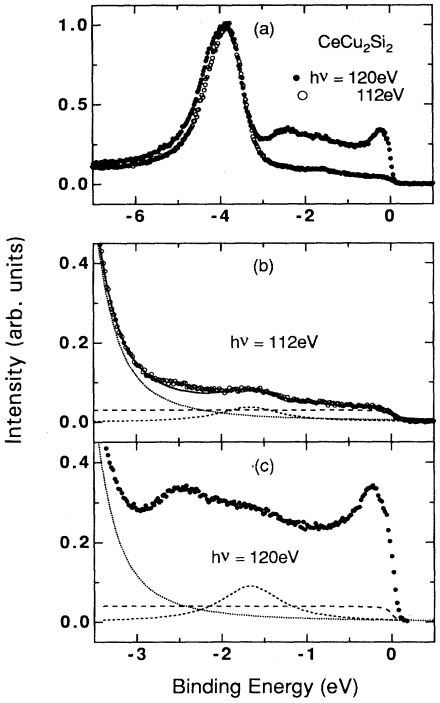

FIG. 8. (a) The on-resonance ($h\nu = 120$ eV) and off-resonance ($h\nu = 112$ eV) spectra of $CeCu_2Si_2$ at $T = 80$ K, normalized to unity at the Cu emission peak at 4 eV. (b) The off-resonance spectrum, fit to the sum of (i) a Lorentzian (dotted line) with $E_B = 3.7$ eV and FWHM $= 0.58$ eV, representing the tail of the Cu emission peak; (ii) a Lorentzian (medium-dashed line) with $E_B = 1.66$ eV and FWHM $= 0.86$ eV, representing the $5d$ emission; and (iii) a reversed arctangent with width 0.5 eV (long-dashed line) representing the Fermi step. The solid line is the sum of the three contributions. A small amount of $4f$ emission is apparent near 2.5 eV. (c) The on-resonance spectrum. The three fit curves are the same as in (b), only enhanced as explained in the text to give a non-$4f$ contribution to the valence band of 30%, as for the other compounds.

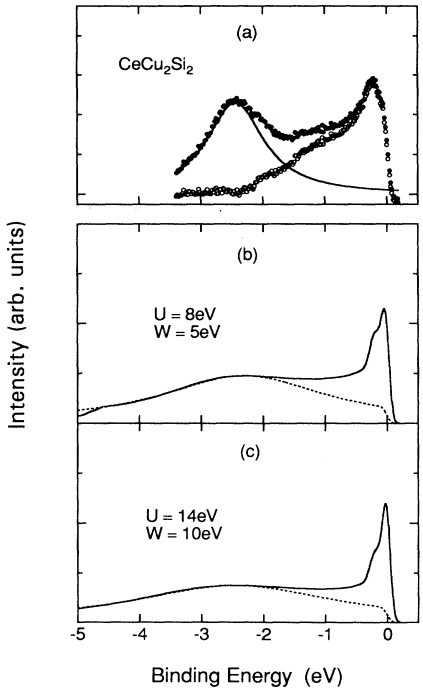

FIG. 9. (a) The $4f$ emission for $CeCu_2Si_2$ (solid circles) obtained after subtracting the fit curves of Fig. 8(c) from the total spectrum. The parameters of the $4f^1$ Lorentzian are $E_B = 2.44$ eV and FWHM $= 1.12$ eV. The open circles are the remaining near-ε_F emission, after subtraction of the Lorentzian. (b) Calculation of the $4f$ emission for $CeCu_2Si_2$ for $W = 5$ eV and $U = 8$ eV. (c) Calculation of the spectrum assuming $W = 10$ eV and $U = 14$ eV. (For further explanation of the theory curves, see the caption for Fig. 10 and the text of Sec. V.)

basis states [(5.17), (5.18), and (5.20)] have been modified to include the splitting of the f^1 configuration into multiplets. The set of coupled equations for the resolvent can be separated by using a decoupling approximation similar to that used in Ref. 13. The decoupling approximation is essentially the same as the one that occurs in the calculation of the ground state, and is also expected to produce reasonable results in the limit $U \gg W$. The photoemission spectrum is then obtained by taking matrix elements of the resolvent and the state in which an f electron has been removed from the ground state. The resulting expression for the one-electron removal spectrum contains factors which depend on both the proportions of the f^1 and the f^2 configuration in the ground state, as well as cross terms.

For energies within T_K of the Fermi level ε_F, the only contribution to the spectrum comes from a Dirac δ-function component of the resolvent. In this energy regime, the integral over the Dirac δ function can be performed and the photoemission spectrum is of the form of Eq. (5.30) of Ref. 13. However, use of the same large U/W approximation as made in the decoupling procedures described above, removes the integrals to yield the analytic expression

$$I(\omega)=\mathfrak{N}^{-4}\sum_{\{\alpha\}}[U/(U+E_f-\varepsilon_F)]^2(a_{\mathbf{k},\{\alpha\}}-(N_{\{\alpha\}}\Delta/\pi)^{1/2}[U/(U+E_f-\varepsilon_F)^2] \otimes\sum_{\{\beta\}}(N_{\{\beta\}}\Delta/\pi)\{[1/(E_{f\{\beta\}}-E_f+k_BT_K)]-[1/(W+\varepsilon_F)]\})^2 , \quad (1)$$

where $\mathfrak{N}$ is the renormalization of the ground state, $E_f<0$ for cerium, $\Delta=V^2\rho$, and $a_{\mathbf{k},\{\alpha\}}$ depends on $e_{\mathbf{k}}=\hbar\omega+\mu$ through the relation

$$a_{\mathbf{k},\{\alpha\}}=-(N_{\{\alpha\}}\Delta/\pi)^{1/2}[(U+2\Gamma)/(U+2\Gamma+E_f-\varepsilon_F)]\otimes(E_{f\{\alpha\}}-E_f+\varepsilon_F-e_{\mathbf{k}}+T_K)^{-1} . \quad (2)$$

Here, $\Gamma\cong(14\Delta/\pi)(W/U+E_f-\varepsilon_F)$ is small (for $\Delta=0.1$ eV it is of order 0.4 eV) relative U. Each multiplet contributes three terms to the photocurrent. The first, proportional to $a^2_{\mathbf{k},\{\alpha\}}$, is already present for $U=\infty$; it represents the rising tail of the ground multiplet, crystal-field, or spin-orbit Kondo resonance, with apparent divergence above ε_F at kT_K, $\Delta_{CF}+kT_K$, or $\Delta_{SO}+kT_K$, respectively. Physically, these tails represent the energy distribution of the conduction electrons involved in the screening of the f moment. It is seen that the inclusion of the f^2 component leads to the addition of an energy-independent constant to the photoemission amplitude near the Fermi level, as evidenced by the last term in the bold parentheses of Eq. (1). Finally, cross terms give rise to a weakly energy-dependent constructive interference, which is smaller by a factor $\Delta/(U+E_f)$ than the leading term for the tail of the resonance. (The situation is very similar to Fig. 3 of Ref. 13, except that there are separate contributions for each multiplet.)

For energies further away from the Fermi energy, both the Dirac δ function and the continuum part of the resolvent contribute terms to the spectrum. The resulting convolution is evaluated numerically. The calculated spectrum has features similar to those found by Bickers, Cox, and Wilkins[2] in their evaluation of the f electron density of states for the $U\rightarrow\infty$ limit of the single-impurity Anderson model in the noncrossing approximation (NCA). That is, the spectrum has a broad continuum of f states stretching down at least to the lower edge of the conduction band. The precise shape, including the width and peak energy position, is strongly influenced by the choice of the conduction-band density of states, and the magnitude of the width $W+\varepsilon_F$ of the occupied portion of the conduction band. Closer to the Fermi energy, the spectrum shows Kondo sidebands, due to the existence of the Kondo spin singlets involving the higher energy f^1 multiplets. In the theory, these split Kondo singlet states may occur as final states.

In addition to the features that are also found in the $U\rightarrow\infty$ NCA calculation,[2] the present calculation has a component due to the f^2 configuration in the ground state. This component produces the constructive interference in the spectrum near the Fermi energy as mentioned above. The f^2 component can also lead to the result that the spectrum has spurious structure at energies of order $(U+2E_f-2\varepsilon_F)$, below the Fermi energy ε_F, if $U+2E_f-2\varepsilon_F\neq 0$. We have ignored this feature, for reasons which we will outline in a future review.

V. THE CALCULATED SPECTRA

To carry out the calculations, certain parameters must be determined in a manner consistent with the known properties of the four Ce compounds. A key parameter is the Kondo temperature, which can be determined from experimental data in one of several ways. Use of the known coefficients of specific-heat γ (Refs. 14–16) and the Bethe-Ansatz formula[17] $T_K=\pi R/6\gamma$ gives $T_K=3.6$, 7.2, and 42 K for $CeAl_3$, $CeCu_2Si_2$, and $CeSi_2$, respectively. Use of the rule[18] that T_K equals the neutron-scattering quasielastic linewidth ω_0 gives $T_K=6$, 6–10, 48, and 290 K for $CeAl_3$, $CeCu_2Si_2$, $CeSi_2$, and $CeBe_{13}$, respectively.[19–22] Use of the rule[2] that $T_K\cong 3.5T_{max}$, where T_{max} is the temperature of the broad maximum in susceptibility in mixed valent compounds gives $T_K=490$ K for $CeBe_{13}$.[23] We therefore set $T_K=4$, 8, 40, and 400 K for the four compounds. (In Ref. 15, inclusion of an extra factor of π in the formula relating T_K and γ leads to a correspondingly larger value of T_K for $CeSi_2$. Our choice gives consistency between the value deduced from γ and that deduced from ω_0.) Next, the crystal-field splittings are set at 5 and 8 meV for $CeAl_3$, at 20 and 32 meV for $CeCu_2Si_2$, and at 25 and 48 meV for $CeSi_2$, using neutron-scattering results.[21,22,24] For $CeBe_{13}$ only quasielastic scattering (i.e., no crystal-field excitations) was observed in neutron scattering[20] and the susceptibility[23] has a broad maximum characteristic[2] of mixed valent com-

pounds with orbital degeneracy $N_f=2J+1=6$; hence, the calculation ignored crystal fields and set $N_f=6$. For the spin-orbit splittings, we used the value 0.28 eV for all four cases, as this value is consistent with the splitting observed in higher resolution photoemission spectra[4] and is typical for cerium compounds.

As we will see, a key parameter for determining the spectral weights and f^1 linewidth is the bandwidth of the background conduction band. For all four compounds, the cerium hybridizes with the s,p electrons on the nearest neighbor (Al, Be, or Si). Band calculations[25] for $CeAl_3$ and $CeCu_2Si_2$ show that the bottom of the s,p band lies at a distance $W=9-10$ eV below the Fermi level ε_F. We do not know of calculations for the other two compounds, but calculations for UBe_{13},[26] which should have a similar s,p band to $CeBe_{13}$, give $W=10$ eV; and we assume that the Si s,p band in $CeSi_2$ should have a similar width as in $CeCu_2Si_2$. Therefore we have set $W=10$ eV for all four cases, as this appears to be a characteristic value for compounds of rare earths with these s,p elements. The conduction band is taken as rectangular (constant $\rho=1/2W$) with $\varepsilon_F=0$. We fix the Coulomb correlation energy as $U=14$ eV; this value which is somewhat larger than the accepted value $U=6$ eV, is taken as small as possible, but larger than W since the calculation requires $U>W$, as discussed above.

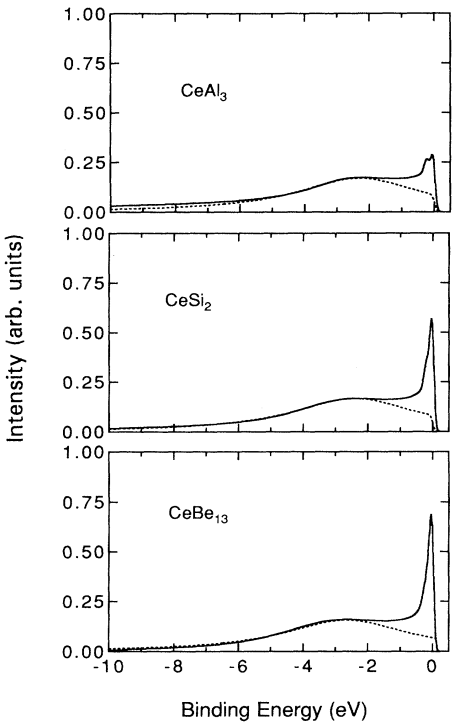

FIG. 10. Calculations of the $4f$ emission for $CeAl_3$, $CeSi_2$, and $CeBe_{13}$ using the low-order $1/N$ expansion of the Anderson impurity model. The bottom of the conduction band is set at $W=10$ eV in accordance with known s,p bandwidths of conventional rare-earth counterparts, and the Coulomb correlation is set at $U=14$ eV. Other parameters are chosen, as described in the text, in accord with experimentally known Kondo temperatures, crystal-field and spin-orbit splittings, and final position of the $f^1\rightarrow f^0$ peak. The dashed lines are Lorentzians, representing the $f^1\rightarrow f^0$ emission; the binding energies are the same as for the experimental case and the widths and spectral weights are given in Table I.

Finally we adjust both the bare value of the energy E_f of the f^1 level and the average hybridization width $\Delta=V^2\rho$ to simultaneously yield the observed ("renormalized") f^1 level energy $\tilde{E}_f$ and the Kondo temperature. Following this we convolute the spectra with the known resolution (150 meV) using a three-point smoothing method (which correctly convolutes δ functions and step functions). The resulting spectra are shown in Figs. 9(c) and 10. To determine the $f^1\rightarrow f^0$ linewidth and the relative spectral weights in the two peaks, we fit the high binding energy part of the spectra to Lorentzians [dashed lines in Figs. 9(c) and 10] in precisely the same manner as for the experimental spectra. The resulting linewidths and fractional weights in the near-ε_F peaks are given in Table I where it can be seen that the experimental widths of the $f^1\rightarrow f^0$ peaks are three to five times narrower than the theoretical widths, and the fractional weight in the near-ε_F peak is 1.65, 1.85, and 2.33 times greater in the experimental spectra for $CeSi_2$, $CeAl_3$, and $CeCu_2Si_2$ than in the theoretical spectra; for $CeBe_{13}$ the agreement is much better.

Somewhat better agreement with experiment can be obtained by choosing a more realistic value of U (8 eV) but a less realistic value of W (5 eV). The results are shown in Figs. 9(b) and 11 and Table I. For $CeSi_2$ and $CeBe_{13}$ the fractional weights in the near-ε_F peaks are closer to the experimental values; however, the theory continues to give too little weight for $CeAl_3$ and $CeCu_2Si_2$ and too large a value for the width of the $f^1\rightarrow f^0$ excitation for all four compounds.

VI. DISCUSSION

Comparison of the experimental $4f$ spectra [Figs. 2(b), 4(c), 7(b), and 9(a)] to the theoretical spectra (Figs. 9–11) show that on the scale of the bandwidth and for the resolution utilized here, the theory underestimates the spectral weight in the near-ε_F peak, and it overestimates the width of the main $f^1\rightarrow f^0$ peak (see also Table I). Visual comparison of the spectra for $CeCu_2Si_2$ in Fig. 9 makes this particularly clear. Reduction of U, with a concomitant reduction of W, can improve the fractional weights somewhat, but overall agreement remains visually poor.

We note in passing that our spectrum, taken for a cleaved single crystal of $CeCu_2Si_2$ at resolution ~ 150 meV, is significantly different from the low resolution (~ 600 meV) spectrum[27] of polycrystalline $CeCu_2Si_2$ used recently by Kang *et al.*[28] Adding additional rounding to our spectra to simulate 600 meV resolution does not remove the discrepancy, which is mainly that our data show more weight in the near-ε_F peak than do the older data. It is our experience that single-crystal data are more reliable. Thus, the analysis of Ref. 28 needs to be reconsidered.

The experimental $f^1\rightarrow f^0$ line widths all have comparable magnitude and also are comparable to those of normal rare-earth core levels (for example, the $4f$ level of

TABLE I. Widths of the f^1 Lorentzian and ratio of the spectral weight in the near-ε_F emission to the total $4f$ emission for the experimental spectra and for the theoretical spectra of Figs. 9–11. The values given for the experimental spectral weight are lower limits; subtraction of surface emission would decrease the relative $f^1 \rightarrow f^0$ weight. The parameters W and U used in the calculation are given for each case, as are E_f (bare f-level energy) and Δ, which are adjusted to yield the experimental ("renormalized") f-level energy $\hat{E}_f$ and Kondo temperature T_K. All energies are given in eV.

	Experiment		Theory			
	Width FWHM $f^1 \rightarrow f^0$	Fractional weight near ε_F	Width FWHM $f^1 \rightarrow f^0$		Fractional weight near ε_F	
$CeAl_3$	0.9	>37%	$W=10$	$U=14$	$E_f=-2.65$	$\Delta=0.0942$
			4.7		20%	
$T_K=4$ K	$\hat{E}_f=-2.20$		$W=5$	$U=8$	$E_f=-2.00$	$\Delta=0.0750$
			2.5		24%	
$CeCu_2Si_2$	1.1	>49%	$W=10$	$U=14$	$E_f=-2.70$	$\Delta=0.1057$
			4.0		21%	
$T_K=8$ K	$\hat{E}_f=-2.45$		$W=5$	$U=8$	$E_f=-2.20$	$\Delta=0.0893$
			3.3		25%	
$CeSi_2$	1.5	>33%	$W=10$	$U=14$	$E_f=-2.70$	$\Delta=0.1136$
			4.7		20%	
$T_K=40$	$\hat{E}_f=-2.35$		$W=5$	$U=8$	$E_f=-2.20$	$\Delta=0.0914$
			3.5		30%	
$CeBe_{13}$	1.2	>28%	$W=10$	$U=14$	$E_f=-2.75$	$\Delta=0.1247$
			4.7		24%	
$T_K=400$ K	$\hat{E}_f=-2.60$		$W=5$	$U=8$	$E_f=-1.95$	$\Delta=0.0987$
			3.4		32%%	

$PrAl_3$ in Fig. 3 has a FWHM of 1.5 eV; the Lorentzian component of the $4f$ spectra for $PrBe_{13}$ has a FWHM of 1.2 eV). Such small observed linewidths are disturbing in that the prediction of a large hybridization width (essentially 28Δ FWHM) for the $f^1 \rightarrow f^0$ transition is one of the most basic features of the model. [Kang *et al.*[28] calculate a narrow width for $CeCu_2Si_2$ by ignoring crystal-field splitting; in the calculation they use $\Delta \cong 0.06$ eV. For our calculation, where crystal-field splitting is not ignored, a larger value of Δ (0.09–0.10 eV) is required to reproduce T_K; hence, our value of the $f^1 \rightarrow f^0$ width is also larger.] It is as though the decay of the $4f$ core hole (which, given the narrow experimental width, is *slower* than predicted) has nothing to do with hybridization. Concerning the spectral weights, not only are the theoretical predictions too small, but the systematics are wrong. The theory predicts (Table I) a nearly linear increase in the near-ε_F spectral weight as the hybridization Δ increases at fixed W and U; but the data show an *inverse* correlation between Δ and spectral weight near the Fermi level.

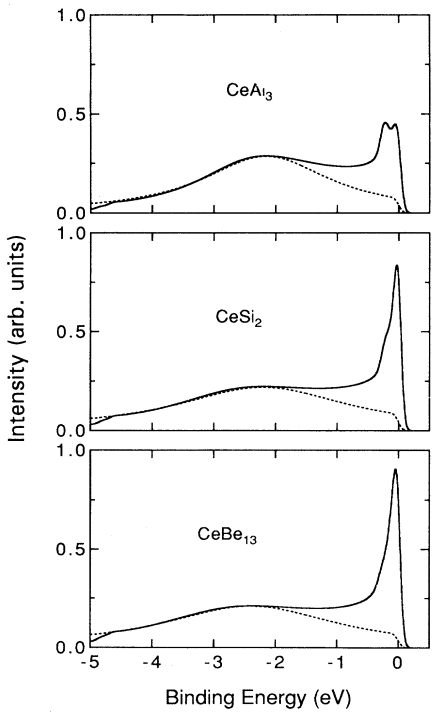

FIG. 11. Same as Fig. 10, but with $W=5$ eV and $U=8$ eV.

The question is, how significant are these disagreements? On the one hand, the calculation does fit the data to within an order of magnitude. Furthermore, the Anderson model is simply that—a *model* which is designed to give the correct low-energy behavior (which behavior exhibits universality, and hence has a certain degree of independence of the high-energy details), but which perhaps should not be expected to give good agreement on large energy scales. From this point of view, a prediction of two peaks with the correct order of magnitude for the widths and weights is sufficient. Of course, such a relaxed requirement would apply equally to any competing model of cerium photoemission. On the other hand, a good deal of emphasis[2–4] has been given as to the degree to which the predictions of the model fit the experimental photoemission spectra. In addition, we wish to know whether the model ignores any fundamental physics; in particular, whether final-state Coulomb screening and banding effects play a more significant role in the spectra than implied by use of the impurity model. For

these reasons, we take the disagreements seriously; and in what follows, we examine several experimental and theoretical problems which will need to be resolved in order to make progress on these issues.

On the experimental side we first consider the method of determining the non-4f background. There are at least three methods that are widely used. The first[1] is to compare spectra taken on (120 eV) and off (112 eV) the giant 4d resonance; the second[3] is to compare spectra taken above (e.g., at $h\nu=40$ eV) and below (e.g., at $h\nu=20$ eV) the presumed threshold (near $h\nu=30$ eV) for the onset of Ce 4f emission; the third is to compare the emission for the Ce compound to that of a La compound. As we have shown, the first method ignores the fact that the 5d electrons contribute at least 30% of the spectrum at 120 eV. Applying this approach to $CeCu_2Si_2$, by simply subtracting the two spectra in Fig. 8(a), gives a non-4f fraction of 17%; it also leaves a significant peak at 1.67 eV in the resulting spectrum, which we believe is due to non-4f emission, rather than 4f emission as implied by this method. The second method can underestimate the amount of 4f emission at 20 eV (it does not actually vanish) and 5d emission at 40 eV. The third (which is the method we use) overlooks possible differences between the Ce and La 5d spectra.

All three methods require additional input as to how to correctly normalize between comparison spectra. We have chosen to normalize our spectra to core levels wherever possible; in doing so we have ignored possible photon energy dependence of the core-level emission over the limited range 116–126 eV. An alternative method is to normalize to incident photon flux (by measuring mesh current); however, in polycrystals this can give very bad results, due to unpredictable cleave dependencies.

A second source of uncertainty is that the photon energy dependence of the matrix elements for optical absorption may differ for different energy regions of the 4f spectrum. In particular, the branching ratio of the near-ε_F peaks to the $f^1\rightarrow f^0$ peak may vary with photon energy; indeed, this is known to occur in the vicinity of the 4d resonance.[29,30] Examination of Fig. 5 demonstrates clearly that the branching ratio for the 5d states varies considerably between 26 and 120 eV. Hence, there is no *a priori* reason for assuming that the 4f branching ratio is constant over any energy range. This means that the spectrum taken at a particular photon energy may not be simply proportional to the spectral density.

At the photon energy that we use (120 eV) the spectra are highly surface sensitive. In our analysis, however, we have ignored the distinction between surface and bulk emission. Recently it has been shown[31] that the surface emission occurs primarily in the $f^1\rightarrow f^0$ peak near 2 eV. For the compound $CeRh_3$ (which has a very large $T_K>1000$ K) there is substantial weight in the 2-eV feature at 120 eV, but spectra[6] taken at $h\nu=884$ eV show very little weight in the $f^1\rightarrow f^0$ peak. The argument is that for the larger photon energy the spectra should be dominated by bulk emission. If all this is true, then were we to account for surface emission in our spectra, there would be *less* weight in the bulk 2-eV feature, and hence the fractional weight in the near-ε_F peak would be even larger than our results suggest. In that sense, our results are lower limits for the fractional spectral weight. Hence, the disagreement with theory is even greater than we have stated above. It should be pointed out that, given the lack of knowledge of the 4f branching ratio discussed above, it is possible that some of the differences between the 120- and 884-eV spectra may not be due to such a surface effect.

The greatest uncertainty in theoretical spectra arises from the lack of knowledge of the energy dependence of the combined hybridization matrix element and conduction-band density of states $\Delta(E)=V^2(E)\rho(E)$. The line shape of the 4f spectrum over the full energy range is extremely sensitive to the choice of the energy dependence of this parameter. (For this reason, it is all the more surprising that the $f^1\rightarrow f^0$ peak observed experimentally is for all compounds a Lorentzian with FWHM$\cong$1 eV.) We have chosen to ignore the energy dependence [$\Delta(\varepsilon)=\Delta$ independent of energy] and have chosen to cut the conduction band off 10 eV below the Fermi level, since this seems to be the appropriate bandwidth for compounds of rare earths with the s,p elements Al, Be, and Si. A smaller choice of bandwidth causes more f^2 weight to pile up near the Fermi energy and changes the ratio of near-ε_F emission to 2-eV emission. In addition, if the bandwidth is made so small that the bare 4f level resides close to the bottom of the band, then the $f^1\rightarrow f^0$ line shape alters dramatically. [In an earlier $U=\infty$ NCA calculation[3] for $CeSi_2$, the background band was assumed to be Gaussian, with a small bandwidth (3 eV FWHM); the final f level is pushed well out in the tail where the density of states is low and hence the hybridization is weak. For this choice of band shape, the resulting $f^1\rightarrow f^0$ width is small and comparable to experiment. However, in our opinion, this is a very unrealistic choice of band shape for $CeSi_2$, and it strengthens our point that fits in the literature are strongly dependent on the choice of $\Delta(E)$, which is essentially unknown.] A variety of recent studies[28,32–35] attempt to derive $\Delta(E)$ and other parameters of the model from first-principles local-density approximation (LDA) electronic structure calculations. However, there is no general consensus on how to achieve this, since there is uncertainty about the extent to which the LDA already includes the many-body effects which are to be calculated from the resulting model. The issues at hand (concerning the line shape on the scale of the bandwidth) cannot be resolved without solution of this problem.

A second source of uncertainty is the convergence of the large N expansion and the degree to which the truncated expansion adequately represents the spectrum of the Anderson impurity model. Furthermore, the generalization from the infinite U limit to the finite values of U also raises questions; this generalization does not include the effects of configurations f^n with $n>2$, and the nature of the errors introduced by the decoupling approximation remains unknown.

Given all this, the possibility remains that adequate treatment of the photoemission spectra may require inclusion of other physics. Coulomb screening of the final-state hole has been utilized in an attempt to explain the

large differences between Kondo temperatures determined from thermodynamic measurements and alternatively from the photoemission spectra.[36] In addition, it is known that in certain limits a two-peaked spectrum ("well-screened" and "poorly screened" final states) is expected when such screening is present.[37,38] When such screening is added to the Anderson model, the relation between high-energy scales and low-energy scales is known to be affected.[39] A possibility is that some of the extra weight that we observe in the near-ε_F peak arises from this source. It is very probable that the extra *width* in the near-ε_F peak, which is apparent in higher resolution spectra,[4,5] arises from this source. In this regard the extra f emission seen in $PrBe_{13}$ [Fig. 6(b), long-dashed line] is suggestive. Similar peaks in several other Pr compounds[40–42] have been interpreted as evidence for the existence of two final-state screening channels. Indeed, the existence of two $4f$ peaks in Pr compounds with large hybridization (as estimated by the large Kondo temperatures $T_K > 100$ K of the corresponding Ce compounds) now appears to be more the rule than the exception; and this supports the view that the second peak cannot be universally obtained from the Anderson model as suggested in Refs. 1 and 8.

Finally, we raise the possibility that the enhanced spectral weight at the Fermi level, which approaches 50% in these compounds, may mean that the Ce compounds reside closer to the band limit than is implied by use of an essentially local impurity model.[9,10] In this approach, the 2-eV peak would arise in the same way as the 6-eV satellite in nickel. While the physics of this satellite still involves the Coulomb correlation, there are significant differences in the way this approach (as opposed to the Anderson model approach) generates the satellite.[43–46] The possibility that the band limit is more appropriate is supported by the recent work[6] mentioned above for $CeRh_3$ where subtraction of surface emission so drastically reduces the weight in the 2-eV peak that the resulting spectrum is simply that expected for an f band. While the compounds studied here have smaller Kondo temperatures than that of $CeRh_3$, it is quite plausible that correct subtraction of the surface peak would lead to spectra with a much larger peak at ε_F and a much smaller satellite at 2 eV.

All of this suggests that photoemission in cerium compounds is very much an open problem, and that future work, both experimental and theoretical, is in order. On the experimental side, the greatest need is for use of high-quality, well characterized single-crystal surfaces. Studies[6,31] over a broad range of photon energies, coupled with studies of the take-off angle dependence of the emission, are needed to help determine the degree of surface and bulk contribution to the spectra. For similar reasons studies of the photon energy dependence of both the $4f$ and non-f emission over a broad (20–1000 eV) photon energy range in both Ce and related La and Pr compounds are needed to determine the non-f emission and the $4f$ branching ratios. Further thought should be given to normalization. Ongoing improvements[3] in experimental resolution can also be expected to be important.

On the theoretical side, the problem of determining the parameters of the model [such as $\Delta(\varepsilon)$] from first principles presents an important and difficult challenge.[32–35] Improvements in our understanding of the effect of approximations on the predictions of the Anderson model would also be helpful; in this regard, the recent Monte Carlo work[47] is very promising. Further work to assess the importance of Coulomb screening and to determine its effect on the predictions of the Anderson model is necessary.[36–39] Finally, use of many-body theories which use band theory as a starting point may well be necessary to understand valence-band photoemission in cerium compounds.[9,10,34,35,43–46]

ACKNOWLEDGMENTS

We thank J. L. Smith of Los Alamos for providing samples of $PrBe_{13}$. We thank J. Tang of U. C. Irvine and S. List of Texas Instruments, for participating in the data collection. We thank J. W. Allen and D. L. Cox for exchange of information and for useful discussions. Experiments performed at the Brookhaven NSLS were performed under the auspices of the U.S. Department of Energy, as was work performed at Los Alamos. Support for J.M.L. was provided by the joint U. C./Los Alamos INCOR Program and by the Center for Materials Science at Los Alamos.

[1] J. W. Allen, S.-J. Oh, O. Gunnarson, K. Schonhammer, M. B. Maple, M. S. Torikachvili, and I. Lindau, Adv. Phys. **35**, 275 (1986).

[2] N. E. Bickers, D. L. Cox, and J. W. Wilkins, Phys. Rev. B **36**, 2036 (1987).

[3] F. Patthey, J.-M. Imer, W.-D. Schneider, H. Beck, Y. Baer, and B. Delley, Phys. Rev. B. **42**, 8864 (1990).

[4] J. J. Joyce, A. J. Arko, J. Lawrence, P. C. Canfield, Z. Fisk, R. J. Bartlett, and J. D. Thompson, Phys. Rev. Lett. **68**, 236 (1992).

[5] J. J. Joyce, A. J. Arko, J. M. Lawrence, J. Tang, P. C. Canfield, R. J. Bartlett, Z. Fisk, J. D. Thompson, and P. S. Riseborough, Solid State Commun. **83**, 551 (1992).

[6] E. Weschke, C. Laubschat, R. Ecker, A. Höhr, M. Domke, G. Kaindl, L. Severin, and B. Johansson, Phys. Rev. Lett. **69**, 1792 (1992).

[7] F. Gerken, J. Barth, and C. Kunz, in *The State of Particle Accelerators and High Energy Physics, Fermilab, 1981,* Proceedings of the Summer School on High Energy Particle Accelerators, edited by R. A. Carrigan, F. R. Huson, and M. Month, AIP Conf. Proc. No. 92 (AIP, New York, 1982), p. 602.

[8] O. Gunnarsson and K. Schönhammer, in *Handbook on the Physics and Chemistry of Rare Earths, Vol. 10–High Energy Spectroscopy,* edited by K. A. Gschneidner, Jr., L. Eyring, and S. Hüfner (North-Holland, Amsterdam, 1987), p. 103.

[9]A. J. Freeman, B. I. Min, and M. R. Norman, in *Handbook on the Physics and Chemistry of Rare Earths, Vol. 10–High Energy Spectroscopy* (Ref. 8), p. 165.
[10]O. Eriksson, R. C. Albers, A. M. Boring, G. W. Fernando, Y. G. Hao, and B. R. Cooper, Phys. Rev. B **43**, 3137 (1991).
[11]C. Gu, X. Wu, C. G. Olson, and D. W. Lynch, Phys. Rev. Lett. **67**, 1622 (1991).
[12]O. Gunnarsson and K. Schönhammer, Phys. Rev. B **28**, 4315 (1983).
[13]O. Gunnarsson and K. Schönhammer, Phys. Rev. B **31**, 4815 (1985).
[14]G. E. Brodale, R. A. Fisher, N. E. Phillips, and J. Flouquet, Phys. Rev. Lett. **56**, 390 (1986).
[15]H. Yashima and T. Satoh, Solid State Commun. **41**, 723 (1982).
[16]M. Ishikawa, H. Yashima, M.Takahashi, T. Satoh, and M. Takigawa, J. Magn. Magn. Mater. **63&64**, 351 (1987).
[17]V. T. Rajan, Phys. Rev. Lett. **51**, 308 (1983).
[18]D. L. Cox, N. E. Bickers, and J. W. Wilkins, J. Appl. Phys. **57**, 3166 (1985).
[19]A. P. Murani, K. Knorr, K. H. J. Buschow, A. Benoit, and J. Flouquet, Solid State Commun. **36**, 523 (1980).
[20]M. Loewenhaupt and E. Holland-Moritz, J. Appl. Phys. **50**, 7456 (1979).
[21]R. M. Galera, A. P. Murani, and J. Pierre, Physica B **156&157**, 801 (1989).
[22]E. Holland-Moritz, W. Weber, A. Severing, E. Zirngiebl, H. Spille, W. Baus, S. Horn, A. P. Murani, and J. L. Ragazzoni, Phys. Rev. B **39**, 6409 (1989).
[23]G. Krill, J. P. Kappler, M. F. Ravet, A. Amamou, and A. Meyer, J. Phys. F **10**, 1031 (1980).
[24]P. A. Alekseev, I. P. Sadikov, I. A. Markova, E. M. Savitskii, V. F. Terekhova, and O. D. Chistyakov, Fiz. Tverd. Tela (Leningrad) **18**, 2509 (1976) [Sov. Phys. Solid State **18**, 1466 (1976)].
[25]J. Sticht, N. d'Ambrumenil, and J. Kübler, Z. Phys. B **65**, 149 (1986).
[26]A. M. Boring, R. C. Albers, G. Schadler, P. Marksteiner, and P. Weinberger, Phys. Rev. B **35**, 2447 (1987).
[27]R. D. Parks, M. L. denBoer, S. Raaen, J. L. Smith, and G. P. Williams, Phys. Rev. B **30**, 1580 (1984).
[28]J.-S. Kang, J. W. Allen, O. Gunnarsson, N. E. Christensen, O. K. Andersen, Y. Lassailly, M. B. Maple, and M. S. Torikachvili, Phys. Rev. B **41**, 6610 (1990).
[29]J. M. Lawrence, J. W. Allen, S.-J. Oh, and I. Lindau, Phys. Rev. B **26**, 2362 (1982).
[30]O. Gunnarsson and T. C. Li, Phys. Rev. B **36**, 9488 (1987).
[31]C. Laubschat, E. Weschke, C. Holtz, M. Domke, O. Strebel, and G. Kaindl, Phys. Rev. Lett. **65**, 1639 (1990).
[32]L. Z. Liu, J. W. Allen, O. Gunnarsson, N. E. Christensen, and O. K. Andersen, Phys. Rev. B **45**, 8934 (1992).
[33]N. Kioussis, B. R. Cooper, and J. M.Wills, J. Appl. Phys. **63**, 3683 (1988).
[34]M. M. Steiner, R. C. Albers, D. J. Scalapino, and L. J. Sham, Phys. Rev. B **43**, 1637 (1991).
[35]A. M. Boring, R. C. Albers, O. Eriksson, and D. D. Koelling, Phys. Rev. Lett. **68**, 2652 (1992).
[36]O. Gunnarsson and K. Schönhammer, Phys. Rev. B **40**, 4160 (1989).
[37]S. H. Liu and K. M. Ho, Phys. Rev. B **28**, 4220 (1983).
[38]P. S. Riseborough, Solid State Commun. **57**, 721 (1986); see also A. C. Hewson and P. S. Riseborough, *ibid.* **22**, 379 (1977).
[39]M. D. Nunez-Regueiro and M. Avignon, Phys. Rev. Lett. **55**, 615 (1985); and in *Theoretical and Experimental Aspects of Valence Fluctuations and Heavy Fermions*, edited by L. C. Gupta and S. K. Malik (Plenum, New York, 1987), p. 133.
[40]R. D. Parks, S. Raaen, M. L. denBoer, Y.-S. Chang, and G. P. Williams, Phys. Rev. Lett. **52**, 2176 (1984).
[41]D. M. Wieliczka, C. G. Olson, and D. W. Lynch, Phys. Rev. Lett. **52**, 2180 (1984).
[42]G. Kalkowski, E. V. Sampathkumaran, C. Laubschat, M. Domke, and G. Kaindl, Solid State Commun. **55**, 977 (1985).
[43]L. C. Davis and L. A. Feldkamp, Solid State Commun. **34**, 141 (1980).
[44]G. Treglia, F. Ducastelle, and D. Spanjaard, Phys. Rev. B **21**, 3729 (1980); J. Phys. (Paris) **43**, 341 (1982).
[45]A. Liebsch, Phys. Rev. B **23**, 5203 (1981).
[46]P. S. Riseborough, J. Phys. Chem. Solids **52**, 1397 (1991).
[47]R. N. Silver, J. E. Gubernatis, D. S. Sivia, and M. Jarrell, Phys. Rev. Lett. **65**, 496 (1990).